PROCEEDINGS OF SCIENCE

The dynamic range of the upgraded surface-detector stations of AugerPrime

Gioacchino Alex Anastasi[a,*] **for the Pierre Auger Collaboration**[b]

[a] *University of Catania & INFN, Sezione di Catania, Via Santa Sofia 64, Catania, Italy*
[b] *Observatorio Pierre Auger, Av. San Martín Norte 304, 5613 Malargüe, Argentina*

Full author list: https://www.auger.org/archive/authors_icrc_2023.html

E-mail: spokespersons@auger.org

The detection of ultra-high-energy cosmic rays by means of giant detector arrays is often limited by the saturation of the recorded signals near the impact point of the shower core at the ground, where the particle density dramatically increases. The saturation affects in particular the highest energy events, worsening the systematic uncertainties in the reconstruction of the shower characteristics. The upgrade of the Pierre Auger Observatory, called AugerPrime, includes the installation of an 1-inch Small PhotoMultiplier Tube (SPMT) inside each water-Cherenkov station (WCD) of the surface detector array. The SPMT allows an unambiguous measurement of signals down to about 250 m from the shower core, thus reducing the number of events featuring a saturated station to a negligible level. In addition, a 3.8 m^2 plastic scintillator (Scintillator Surface Detector, SSD) is installed on top of each WCD. The SSD is designed to match the WCD (with SPMT) dynamic range, providing a complementary measurement of the shower components up to the highest energies. In this work, the design and performances of the upgraded AugerPrime surface-detector stations in the extended dynamic range are described, highlighting the accuracy of the measurements. A first analysis employing the unsaturated signals in the event reconstruction is also presented.

38th International Cosmic Ray Conference (ICRC2023)
26 July – 3 August, 2023
Nagoya, Japan

*Speaker

PoS(ICRC2023)343

1. Introduction

The Surface Detector (SD) of the Pierre Auger Observatory comprises about 1600 water-Cherenkov detectors arranged in an 1.5 km triangular grid over an area of ~3000 km^2. Extensive air-showers are measured by recording the signals and arrival times of the secondary particles at the ground level, which spread over areas larger than 15 km^2 for primary energies above 3 EeV. The Cherenkov light produced by the shower particles in each WCD are collected by three 9-inch Photonis XP1805 photomultipliers (Large PMTs, LPMTs), for which each input is split in two channels, one amplified (High Gain) with a factor of 32 with respect to the other (Low Gain). Such gain ratio is required to achieve a dynamic range of measurement varying from very low signals generated by single atmospheric muons (used to calibrate the detector), to small signals produced by few shower particles reaching the stations far from the impact point of the shower core at the ground, up to hundreds of thousands of particles in the station closest to the core.

When the distance between the detector and the shower core is shorter than a few hundred meters, the dynamic range turns out to be insufficient to record the signal produced by the huge amount of secondary particles hitting the WCD, which is then tagged as saturated. The saturation initially appears only in the digitized signal traces, as it is due to the FADCs overflow. An actual saturation of the photomultiplier is instead observed when extreme amounts of light reach the LPMTs photocathodes, resulting in a deviation from the linear response. A recovery procedure [1] was implemented to estimate the loss of signal due to saturation. However, when the photomultiplier saturation comes into play, the accuracy of the recovered signal can be worse than 50% and a better estimation can only be obtained with a detailed knowledge of each of the 5000 LPMTs responses in the non-linear region, a non feasible solution.

The measured SD energy estimator S(1000), which is proportional to the density of particles at 1 km from the shower axis, is almost not affected by the presence of a saturated station in the event. On the contrary, its resolution, as shown in Ref. [2], worsens from 3% to about 7% when saturation is present.

In the last years the Pierre Auger Collaboration started an upgrade of the Observatory, called AugerPrime [3, 4], of which the main aim is the collection of new observables sensitive to the nuclear mass of the primary UHECRs. The upgrade consists of several new detectors added to the SD stations, which provide complementary measurements of the shower particles at the ground and thus will allow to disentangle the muonic and electromagnetic components of the showers in combination with the WCD. At the same time, the new detectors are designed to extend the dynamic range of the SD acquisition by more than a decade, recording signals at least as close as 250 m from the shower core without saturation, thus considerably increasing the fraction of events that can be reconstructed unambiguously, i.e. with a complete signal in all stations, up to the highest energies.

2. The AugerPrime upgraded station

The upgraded SD station is equipped with an additional 1-inch diameter photomultiplier (SPMT) installed inside the WCD, a plastic scintillator (SSD) and a radio antenna placed on top of the tank. An underground muon detector is deployed aside the WCDs in a limited area of the array, where the spacing between stations is reduced to 750 m. Moreover, a new electronics (Up-

graded Unified Board, UUB) is installed in each station to process the signals collected by all the detectors, with improved performances and data processing capabilities; a detailed description can be found in Ref. [5]. The added components use the existing communication system and powering infrastructure, except for the substitution of the solar panels to satisfy the increased power-budget demand. Starting from the end of 2020, an increasing part of the SD array has been systematically upgraded with the installation of the UUBs together with the SPMTs and SSD PMTs. During this period the monitoring, acquisition and reconstruction pipelines have been updated to integrate the measurements from the AugerPrime detectors in the data-taking scheme, assessing their conformity to the design requirements. The deployment has been completed in July 2023, and a report on the status and performances can be found in Ref. [6].

The Small PMT. A small 1-inch diameter Hamamatsu R8619 photomultiplier is installed in each WCD exploiting a hitherto unused and easily accessible 30 mm window on the Tyvek bag containing the ultra-pure water. A detailed description of the design and validation tests can be found in Refs. [7, 8] and references therein.

The direct calibration with atmospheric muons employed for the LPMTs is not feasible for the SPMT, due to its photocathode dimensions. In fact, the light released by a single muon crossing the WCD produces on average ∼90 photoelectrons in the LPMTs, while only ∼1 in the SPMT. For this reason, a procedure of cross-calibration of the SPMT with the LPMTs has been developed. Its goal is to derive the conversion factor from the collected charge measured in ADC channels into a signal expressed in physical units, that for the WCDs of the Pierre Auger Observatory is the *Vertical Equivalent Muon* (VEM), i.e. the signal produced by a vertical muon traversing the tank at its center. The conversion factor β is thus defined as

$$S_{\mathrm{SPMT}} = \beta\, Q_{\mathrm{SPMT}} \tag{1}$$

and it is derived by minimizing the differences between the signal spectra measured by the two typologies of PMTs in the same station. A WCD participates in an extensive air-shower event, and thus transmits the triggered signals, only a few times per day. As a consequence, to effectively perform the cross-calibration, a dedicated selection of signals from local low-energy showers (hereafter called *small showers*) has been implemented in the UUB data acquisition software [9]. Small showers are selected requiring a 2-fold coincidence among the 3 LPMTs above individual thresholds between 350 and 550 ADC counts (depending on the gain of each LPMT). A rate of about 200 events/hour is measured separately in each WCD.

The minimization of the differences between the calibrated signal spectra is performed in a superposition region limited: at the lower end, by imposing a minimum of ∼200 VEM on the LPMTs average, to guarantee a signal in the SPMT large enough to be only marginally affected by statistical fluctuations; at the higher end, by the LPMTs (electronic) saturation. A typical result for one upgraded WCD is shown in the left part of Fig. 1, where the two spectra are superimposed in the region below the LPMTs saturation (starting at around 650 VEM) and an extension of the dynamic range up to about 20,000 VEM is achieved with the SPMT measurements.

In order to follow the daily evolution of the SPMT gain due to the temperature variations, the cross-calibration is performed in an 8-hour sliding window. In this way, a precision in the determination of the cross-calibration factor of ∼2.2% is obtained. An example for one station is shown in the right panel of Fig. 1, where the changes in the cross-calibration factor (which can

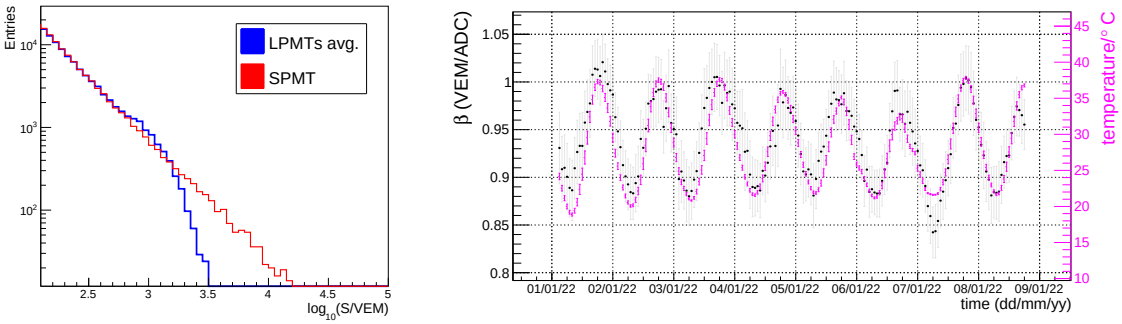

Figure 1: *Left*: Spectra of small showers signals collected in about one month in one upgraded station. *Right*: Cross-calibration factor β for a typical SPMT. The correlation with temperature can be clearly seen.

be as large as ±5% on a daily basis) clearly match the temperature behaviour. The signals from extensive air-showers are eventually calibrated with the nearest β value in time, using the center of each 8-hour interval as a reference.

The Scintillator Surface Detector. The SSD basic unit consists of two scintillator panels, each covering an area of $\simeq 2\,\mathrm{m}^2$, enclosed in a light-tight aluminum box mounted on top of a WCD. Each SSD is equipped with an 1.5-inch bi-alkali Hamamatsu R9420 photomultiplier, located in-between the panels and collecting the light via wavelength-shifting fibers. The output of the SSD PMT is split into two channels, the first one attenuated by a factor 4 (Low Gain) and the second one amplified by a factor 32 (High Gain). This yields a total gain ratio of 128, which allows to cover the required dynamic range. The SSD PMT has been chosen accordingly, being linear within 5% for peak currents up to 160 mA (for a gain of 8×10^4). A description of the design and validation tests can be found in Ref. [10] and references therein.

As for the LPMTs, the SSD calibration is performed using the signals of the atmospheric background particles, collected by means of a dedicated trigger [11]. An example of the acquired charge distribution is shown in Fig. 2. Differently from the WCD, muons and electrons deposit on average the same energy in a scintillator, so the reference physical unit for SSD measurements is the MIP, i.e. the signal produced by a *Minimum-Ionizing Particle* vertically crossing the module. Analogously to the VEM, the most probable charge deposited by a MIP is estimated by fitting the second peak of the charge distribution, the first one being due to the integration of the baseline noise when a time window with no particle signals in the SSD is acquired. In fact, in the calibration process the SSD acts as a subordinate and, given its smaller effective area with respect to the WCD, only about 40% of the calibration triggers correspond to a MIP in the SSD. Nonetheless, the "hump" of both SSD and WCD charge distributions is successfully found for ~99% of the acquired histograms.

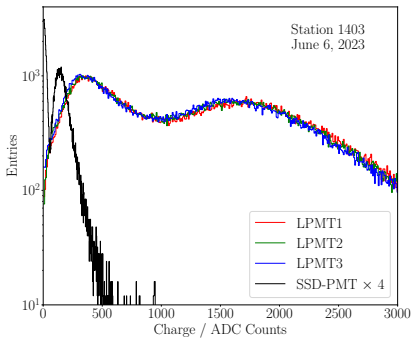

Figure 2: Histograms of VEM and MIP integrated charges, collected in 60 s in one upgraded station.

3. The extended dynamic range

Featuring the same bialkali photocathode of the LPMTs but with an active area ~80 times smaller, the SPMT potentially allows for an equivalent extension of the WCD dynamic range of acquisition. Adjusting its gain in such a way that the ratio of the LPMTs to SPMT signals is limited to a value of ~32, an extension up to about 20,000 VEM can be obtained. With this configuration, the probability of having a saturated station per event is predicted to reduce to a few % even at the highest energies, while in the non-upgraded detector it was as high as ~40% at shower energies of $10^{19.5}$ eV, and further increasing with energy.

At the same time, the SSD provides a complementary measurement of the shower particles at the ground, and the combination with the WCD will allow to disentangle the muonic and electromagnetic components of the showers by exploiting the different responses of the two detectors. In order to benefit the most from the joint information of SSD and WCD measurements, the extended dynamic ranges of both detectors are designed to be similar. For the SSD, this implies to measure non-saturated signals up to ~20,000 MIP.

The correlation between the signals from extensive air-shower events, collected by the two detectors (WCD and SSD) during the deployment period, is shown in the left side of Fig. 3, where both scales are expressed in the corresponding physical units (VEM for the WCD and MIP for the SSD). The signals in the WCDs are measured by the LPMTs up to the saturation (~650 VEM), while above they are derived from the SPMT. The required dynamic range is nicely covered up to the highest particle densities, and the evident correlation allows for a direct cross check between the two detector performances, also demonstrating the validity of the independent calibration procedures.

The increased dynamic range directly impacts the event reconstruction, enhancing the constraining power of the measurements from the station nearest to the shower core in case the LPMT saturation occurs. However, prior to incorporating the new measurements in the reconstruction procedure, the signal accuracy of each of the upgraded detectors has to be quantified.

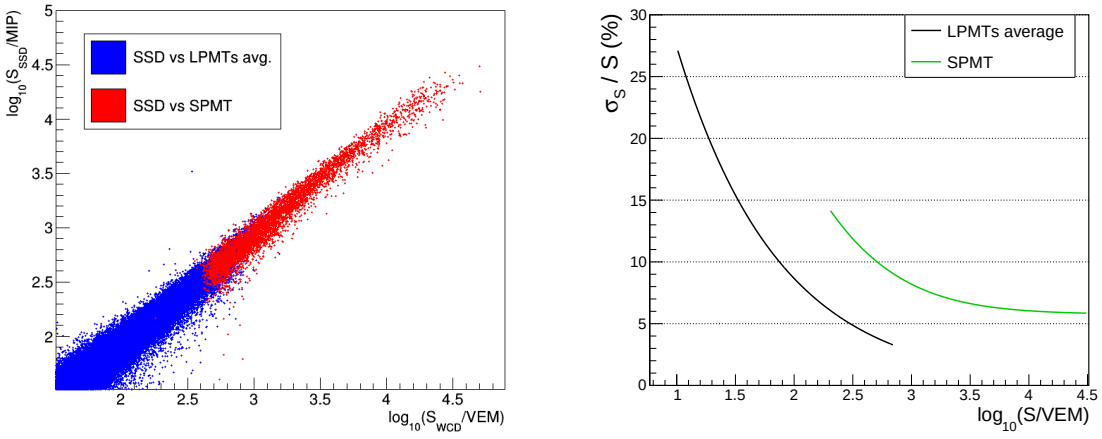

Figure 3: *Left*: correlation of SSD and WCD signals measured in extensive air-shower events. The LPMTs are used up to the saturation (blue dots); the measurements are extended further by means of the SPMT (red dots). *Right*: relative accuracy for the WCD signals as parameterized in Eqs. (2) and (3).

Signal accuracy. A data-driven estimation of the LPMTs signal accuracy is obtained from doublet stations, which have a separation of ∼11 m on the ground. The method is described in Ref. [12] and, applied to the upgraded stations, it provides a Poisson-like parameterization:

$$\sigma_S^2 = f_S^2(\theta)\, S, \quad \text{where} \quad f_S(\theta) = (0.22 \pm 0.09) + (0.55 \pm 0.07)\sec\theta, \tag{2}$$

with θ the zenith angle of the shower.

In the case of the SPMT, very limited statistics has been collected up to now from doublet stations since signals from extensive air-showers in the range of interest (that is above a few hundred VEM) are unavoidably scarce. The SPMT signal accuracy is currently evaluated by comparing the LPMTs and SPMT signals, exploiting the small showers collected for the cross-calibration. In particular, the SPMT signal variance is calculated from the dispersion of the relative differences $(S_{\text{SPMT}} - S_{\text{LPMTs}})/S_{\text{LPMTs}}$ by subtracting the LPMTs accuracy from Eq. (2). The parameterization obtained in the region below the LPMTs saturation is:

$$\sigma_S^2 = f_S^2\, S + c^2\, S^2, \quad \text{where} \quad f_S = (1.8 \pm 0.2)\,,\ c = (0.06 \pm 0.01), \tag{3}$$

which is then extrapolated to higher SPMT signals. For the constant term c, a value compatible with the overall uncertainties in the cross-calibration procedure is obtained. For the Poissonian-like factor f_S, a value at least $\sqrt{3}$ times larger than the LPMTs was actually expected, which corresponds to the difference in the accuracy between the measurements from a single detector (as the SPMT) and the average of 3 detectors (as for the LPMTs average signal). Since the small-shower events are acquired locally in each station, the information on the zenith angle is not available; an evaluation of the zenith dependence is under study by using simulated events.

The accuracy of the WCD PMT measurements is shown in the right plot of Fig. 3. The relative uncertainty on the SPMT signal is lower than 10% when the LPMTs start saturating, and then it rapidly approaches the lower limit of ∼6% dictated by the cross-calibration uncertainty. In a limited region above the saturation of the LPMTs (∼650 VEM) and below ∼1000 VEM, the accuracy of the signals measured by the LPMTs, although saturated, is estimated to be better than the one from the SPMT. Studies on the opportunity of using such signals in the reconstruction are ongoing. On the contrary, for larger signals the SPMT alone delivers unsaturated signals with higher accuracy.

The SSD signal accuracy has been derived from simulations of *pseudo-doublets*, i.e. pairs of stations located at the same lateral distance from the Monte-Carlo simulated shower core but on opposite sides of the shower axis. Also the SSD signal uncertainties are found to be proportional to the square root of the signal, and have been parameterized as

$$\sigma_S^2 = f_S^2(\theta)\, S, \quad \text{where} \quad f_S(\theta) = 1.449 \times [1 + 0.175(\sec\theta - \sec 35^\circ)]. \tag{4}$$

A first comparison with measurements by doublets of SSD detectors showed an agreement roughly within a few percent. Due to the nature of Poisson fluctuations, the relative uncertainty amounts to only a few percent for signals measured within a few hundred meters from the shower axis.

Event reconstruction. The key ingredients in the reconstruction of the arrival direction and of the energy of a shower are: (i) the timing information of the stations, from which the direction of the axis is obtained; (ii) the size of the signals measured in each station, which are fitted as a function

of the distance from the axis to determine the position of the impact point of the core on the ground and the shower size S(1000), the estimator of the primary energy.

At present, the reconstruction of the shower geometry is performed using only the information from the WCD LPMTs and following the well-studied procedure described in Ref. [2]. Then the Lateral Distribution Function (LDF) of the shower is derived by fitting the particle densities measured at each SD station as a function of the distance r to the shower core. A data-driven average LDF in the form $S(r) = S(r_{\rm opt})\, f_{\rm LDF}(r)$ is employed, where $r_{\rm opt}$ is the so-called optimal distance[1] and $f_{\rm NKG}(r)$ a modified Nishimura-Kamata-Greisen function:

$$f_{\rm NKG}(r) = \left(\frac{r}{r_{\rm opt}}\right)^{\beta} \left(\frac{r + r_s}{r_{\rm opt} + r_s}\right)^{\beta+\gamma}, \tag{5}$$

where $r_s = 700\,$m and β, γ are the average slopes, parametrized as functions of shower size and zenith angle. The shower size estimator is defined as the value of $S(r_{\rm opt})$ and, in the case of the Pierre Auger Observatory SD, $r_{\rm opt} = 1000\,$m.

The extension of the procedure to the SSD measurements has been presented in Ref. [13]. The main difference with respect to the traditional reconstruction is that the LDF fit of the SSD signals is performed after fixing the geometry of the shower to the result of the WCD LDF fit. As a consequence, the corresponding uncertainties must be propagated to the SSD signals and added to the signal accuracy from Eq. (4).

An example event, measured with the upgraded SD stations, is shown in Fig. 4. Using the SPMT signal, we are able to constrain the WCD LDF fit down to distances as close as 250 m from the shower core, while only a lower limit (the saturated signal) or a rough estimation (the recovered signal) could be employed before. In this way, a more accurate estimation of S(1000) is obtained and an increased precision in the determination of the shower core is foreseen. In addition, a complementary shower-size estimator from measurements by the SSDs is reconstructed in the same range of particle densities.

4. Summary and Outlook

In the context of the AugerPrime upgrade of the Pierre Auger Observatory, the dynamic range of acquisition of the water-Cherenkov detectors has been extended with the addition of a small diameter photomultiplier, the SPMT, which allows for the measurement of signals without saturation in the vast majority of the observed extensive air-shower events. At the same time, a scintillator detector has been installed on top of each tank, delivering a complementary measurement of the shower particles at ground level. The same dynamic range of the WCD with the SPMT is reached in the SSD by employing a highly-linear photomultiplier and by splitting its output into two channels with a gain ratio of 128.

The first events collected with the array of upgraded stations confirm the effectiveness of this design, allowing the measurement of signals up to at least 20,000 VEM and correspondingly 20,000 MIP without saturation in the digitized traces. As a consequence, the fit of the Lateral

[1]The optimal distance $r_{\rm opt}$ has to be chosen so that the variability in the shower size estimator induced by the shower-to-shower fluctuations is minimized [14].

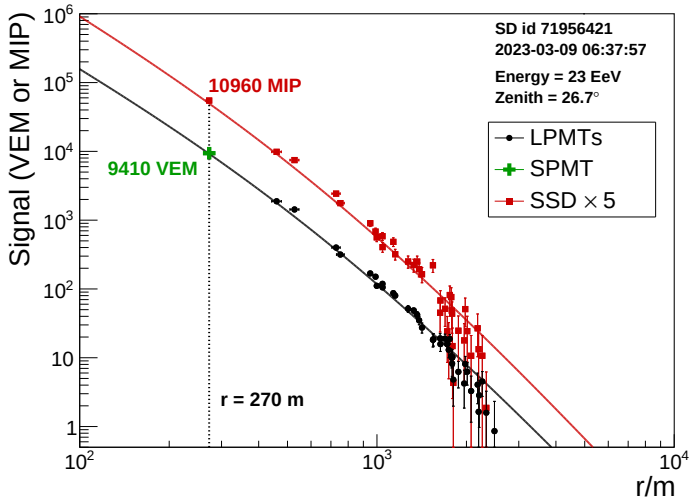

Figure 4: One high-energy event collected by AugerPrime detectors, a 23 EeV shower arriving at a zenith angle of 26.7° and detected with the WCDs (black dots) and SSDs (red squares). In the station nearest to the shower core the LPMTs are saturated, thus the SPMT signal is used (green cross). The SSD signals and SSD LDF are multiplied by a factor 5 for clarity.

Distribution Function can be effectively constrained at least down to distances of about 250 m from the shower core even at the highest energies.

In this configuration, the measurements of the SD will allow to test the modelling of the LDF shape in a range of distances and energies never explored before, reducing the systematic uncertainties in the event reconstruction and in particular in the determination of the shower size, the estimator of the primary energy. Moreover, the studies on the deconvolution of the electromagnetic and muonic shower components, based on the combined information of the WCD and SSD, will benefit from the direct measurement of the shower characteristics in the region near the shower core, where most of the energy is deposited.

References

[1] D. Veberič *et al.* [Pierre Auger coll.], Proc. 33rd Int. Cosmic Ray Conf. [1307.5059].
[2] A. Aab *et al.* [Pierre Auger coll.], JINST 15 (2020) P10021 [2007.09035].
[3] A. Aab *et al.* [Pierre Auger coll.], *The Pierre Auger Observatory Upgrade - Preliminary Design Report* [1604.03637].
[4] A. Castellina *et al.* [Pierre Auger coll.], EPJ Web Conf. 210 (2019) 06002 [1905.04472].
[5] G. Marsella *et al.* [Pierre Auger coll.], Proc. 37th Int. Cosmic Ray Conf., PoS(ICRC2021)230.
[6] F. Convenga *et al.* [Pierre Auger coll.], Proc. 38th Int. Cosmic Ray Conf., PoS(ICRC2023)392.
[7] M. Buscemi *et al.*, JINST 15 (2020) P07011.
[8] G. A. Anastasi *et al.*, JINST 17 (2022) T04003 [2205.11329].
[9] R. Sato *et al.* [Pierre Auger coll.], Proc. 38th Int. Cosmic Ray Conf., PoS(ICRC2023)373.
[10] G. Cataldi *et al.* [Pierre Auger coll.], Proc. 37th Int. Cosmic Ray Conf., PoS(ICRC2021)251.
[11] X. Bertou *et al.*, Nucl. Instrum. Meth. A 568 (2006) 839–846 [2102.01656].
[12] M. Ave *et al.*, Nucl. Instrum. Meth. A 578 (2007) 180-184 [2101.06158].
[13] D. Schmidt *et al.* [Pierre Auger coll.], Proc. 37th Int. Cosmic Ray Conf., PoS(ICRC2021)218.
[14] D. Newton *at al.*, Astropart. Phys. 26 (2007) 414-419 [astro-ph/0608118v1].

The Pierre Auger Collaboration

A. Abdul Halim[13], P. Abreu[72], M. Aglietta[54,52], I. Allekotte[1], K. Almeida Cheminant[70], A. Almela[7,12], R. Aloisio[45,46], J. Alvarez-Muñiz[79], J. Ammerman Yebra[79], G.A. Anastasi[54,52], L. Anchordoqui[86], B. Andrada[7], S. Andringa[72], C. Aramo[50], P.R. Araújo Ferreira[42], E. Arnone[63,52], J. C. Arteaga Velázquez[67], H. Asorey[7], P. Assis[72], G. Avila[11], E. Avocone[57,46], A.M. Badescu[75], A. Bakalova[32], A. Balaceanu[73], F. Barbato[45,46], A. Bartz Mocellin[85], J.A. Bellido[13,69], C. Berat[36], M.E. Bertaina[63,52], G. Bhatta[70], M. Bianciotto[63,52], P.L. Biermann[h], V. Binet[5], K. Bismark[39,7], T. Bister[80,81], J. Biteau[37], J. Blazek[32], C. Bleve[36], J. Blümer[41], M. Boháčová[32], D. Boncioli[57,46], C. Bonifazi[8,26], L. Bonneau Arbeletche[21], N. Borodai[70], J. Brack[j], P.G. Brichetto Orchera[7], F.L. Briechle[42], A. Bueno[78], S. Buitink[15], M. Buscemi[47,61], M. Büsken[39,7], A. Bwembya[80,81], K.S. Caballero-Mora[66], S. Cabana-Freire[79], L. Caccianiga[59,49], I. Caracas[38], R. Caruso[58,47], A. Castellina[54,52], F. Catalani[18], G. Cataldi[48], L. Cazon[79], M. Cerda[10], A. Cermenati[45,46], J.A. Chinellato[21], J. Chudoba[32], L. Chytka[33], R.W. Clay[13], A.C. Cobos Cerutti[6], R. Colalillo[60,50], A. Coleman[90], M.R. Coluccia[48], R. Conceição[72], A. Condorelli[37], G. Consolati[49,55], M. Conte[56,48], F. Convenga[41], D. Correia dos Santos[28], P.J. Costa[72], C.E. Covault[84], M. Cristinziani[44], C.S. Cruz Sanchez[3], S. Dasso[4,2], K. Daumiller[41], B.R. Dawson[13], R.M. de Almeida[28], J. de Jesús[7,41], S.J. de Jong[80,81], J.R.T. de Mello Neto[26,27], I. De Mitri[45,46], J. de Oliveira[17], D. de Oliveira Franco[21], F. de Palma[56,48], V. de Souza[19], E. De Vito[56,48], A. Del Popolo[58,47], O. Deligny[34], N. Denner[32], L. Deval[41,7], A. di Matteo[52], M. Dobre[73], C. Dobrigkeit[21], J.C. D'Olivo[68], L.M. Domingues Mendes[72], J.C. dos Anjos, R.C. dos Anjos[25], J. Ebr[32], F. Ellwanger[41], M. Emam[80,81], R. Engel[39,41], I. Epicoco[56,48], M. Erdmann[42], A. Etchegoyen[7,12], C. Evoli[45,46], H. Falcke[80,82,81], J. Farmer[89], G. Farrar[88], A.C. Fauth[21], N. Fazzini[e], F. Feldbusch[40], F. Fenu[41,d], A. Fernandes[72], B. Fick[87], J.M. Figueira[7], A. Filipčič[77,76], T. Fitoussi[41], B. Flaggs[90], T. Fodran[80], T. Fujii[89,f], A. Fuster[7,12], C. Galea[80], C. Galelli[59,49], B. García[6], C. Gaudu[38], H. Gemmeke[40], F. Gesualdi[7,41], A. Gherghel-Lascu[73], P.L. Ghia[34], U. Giaccari[48], M. Giammarchi[49], J. Glombitza[42,g], F. Gobbi[10], F. Gollan[7], G. Golup[1], M. Gómez Berisso[1], P.F. Gómez Vitale[11], J.P. Gongora[11], J.M. González[1], N. González[7], I. Goos[1], D. Góra[70], A. Gorgi[54,52], M. Gottowik[79], T.D. Grubb[13], F. Guarino[60,50], G.P. Guedes[22], E. Guido[44], S. Hahn[39], P. Hamal[32], M.R. Hampel[7], P. Hansen[3], D. Harari[1], V.M. Harvey[13], A. Haungs[41], T. Hebbeker[42], C. Hojvat[e], J.R. Hörandel[80,81], P. Horvath[33], M. Hrabovský[33], T. Huege[41,15], A. Insolia[58,47], P.G. Isar[74], P. Janecek[32], J.A. Johnsen[85], J. Jurysek[32], A. Kääpä[38], K.H. Kampert[38], B. Keilhauer[41], A. Khakurdikar[80], V.V. Kizakke Covilakam[7,41], H.O. Klages[41], M. Kleifges[40], F. Knapp[39], N. Kunka[40], B.L. Lago[16], N. Langner[42], M.A. Leigui de Oliveira[24], Y Lema-Capeans[79], V. Lenok[39], A. Letessier-Selvon[35], I. Lhenry-Yvon[34], D. Lo Presti[58,47], L. Lopes[72], L. Lu[91], Q. Luce[39], J.P. Lundquist[76], A. Machado Payeras[21], M. Majercakova[32], D. Mandat[32], B.C. Manning[13], P. Mantsch[e], S. Marafico[34], F.M. Mariani[59,49], A.G. Mariazzi[3], I.C. Mariş[14], G. Marsella[61,47], D. Martello[56,48], S. Martinelli[41,7], O. Martínez Bravo[64], M.A. Martins[79], M. Mastrodicasa[57,46], H.J. Mathes[41], J. Matthews[a], G. Matthiae[62,51], E. Mayotte[85,38], S. Mayotte[85], P.O. Mazur[e], G. Medina-Tanco[68], J. Meinert[38], D. Melo[7], A. Menshikov[40], C. Merx[41], S. Michal[33], M.I. Micheletti[5], L. Miramonti[59,49], S. Mollerach[1], F. Montanet[36], L. Morejon[38], C. Morello[54,52], A.L. Müller[32], K. Mulrey[80,81], R. Mussa[52], M. Muzio[88], W.M. Namasaka[38], S. Negi[32], L. Nellen[68], K. Nguyen[87], G. Nicora[9], M. Niculescu-Oglinzanu[73], M. Niechciol[44], D. Nitz[87], D. Nosek[31], V. Novotny[31], L. Nožka[33], A Nucita[56,48], L.A. Núñez[30], C. Oliveira[19], M. Palatka[32], J. Pallotta[9], S. Panja[32], G. Parente[79], T. Paulsen[38], J. Pawlowsky[38], M. Pech[32], J. Pękala[70], R. Pelayo[65], L.A.S. Pereira[23], E.E. Pereira Martins[39,7], J. Perez Armand[20], C. Pérez Bertolli[7,41], L. Perrone[56,48], S. Petrera[45,46], C. Petrucci[57,46], T. Pierog[41], M. Pimenta[72], M. Platino[7], B. Pont[80], M. Pothast[81,80], M. Pourmohammad Shahvar[61,47], P. Privitera[89], M. Prouza[32], A. Puyleart[87], S. Querchfeld[38], J. Rautenberg[38], D. Ravignani[7], M. Reininghaus[39], J. Ridky[32], F. Riehn[79], M. Risse[44], V. Rizi[57,46], W. Rodrigues de Carvalho[80], E. Rodriguez[7,41], J. Rodriguez Rojo[11], M.J. Roncoroni[7], S. Rossoni[43], M. Roth[41], E. Roulet[1], A.C. Rovero[4], P. Ruehl[44], A. Saftoiu[73], M. Saharan[80], F. Salamida[57,46], H. Salazar[64], G. Salina[51], J.D. Sanabria Gomez[30], F. Sánchez[7], E.M. Santos[20], E. Santos[32],

F. Sarazin[85], R. Sarmento[72], R. Sato[11], P. Savina[91], C.M. Schäfer[41], V. Scherini[56,48], H. Schieler[41], M. Schimassek[34], M. Schimp[38], F. Schlüter[41], D. Schmidt[39], O. Scholten[15,i], H. Schoorlemmer[80,81], P. Schovánek[32], F.G. Schröder[90,41], J. Schulte[42], T. Schulz[41], S.J. Sciutto[3], M. Scornavacche[7,41], A. Segreto[53,47], S. Sehgal[38], S.U. Shivashankara[76], G. Sigl[43], G. Silli[7], O. Sima[73,b], F. Simon[40], R. Smau[73], R. Šmída[89], P. Sommers[k], J.F. Soriano[86], R. Squartini[10], M. Stadelmaier[32], D. Stanca[73], S. Stanič[76], J. Stasielak[70], P. Stassi[36], S. Strähnz[39], M. Straub[42], M. Suárez-Durán[14], T. Suomijärvi[37], A.D. Supanitsky[7], Z. Svozilikova[32], Z. Szadkowski[71], A. Tapia[29], C. Taricco[63,52], C. Timmermans[81,80], O. Tkachenko[41], P. Tobiska[32], C.J. Todero Peixoto[18], B. Tomé[72], Z. Torrès[36], A. Travaini[10], P. Travnicek[32], C. Trimarelli[57,46], M. Tueros[3], M. Unger[41], L. Vaclavek[33], M. Vacula[33], J.F. Valdés Galicia[68], L. Valore[60,50], E. Varela[64], A. Vásquez-Ramírez[30], D. Veberič[41], C. Ventura[27], I.D. Vergara Quispe[3], V. Verzi[51], J. Vicha[32], J. Vink[83], J. Vlastimil[32], S. Vorobiov[76], C. Watanabe[26], A.A. Watson[c], A. Weindl[41], L. Wiencke[85], H. Wilczyński[70], D. Wittkowski[38], B. Wundheiler[7], B. Yue[38], A. Yushkov[32], O. Zapparrata[14], E. Zas[79], D. Zavrtanik[76,77], M. Zavrtanik[77,76]

———— • ————

[1] Centro Atómico Bariloche and Instituto Balseiro (CNEA-UNCuyo-CONICET), San Carlos de Bariloche, Argentina
[2] Departamento de Física and Departamento de Ciencias de la Atmósfera y los Océanos, FCEyN, Universidad de Buenos Aires and CONICET, Buenos Aires, Argentina
[3] IFLP, Universidad Nacional de La Plata and CONICET, La Plata, Argentina
[4] Instituto de Astronomía y Física del Espacio (IAFE, CONICET-UBA), Buenos Aires, Argentina
[5] Instituto de Física de Rosario (IFIR) – CONICET/U.N.R. and Facultad de Ciencias Bioquímicas y Farmacéuticas U.N.R., Rosario, Argentina
[6] Instituto de Tecnologías en Detección y Astropartículas (CNEA, CONICET, UNSAM), and Universidad Tecnológica Nacional – Facultad Regional Mendoza (CONICET/CNEA), Mendoza, Argentina
[7] Instituto de Tecnologías en Detección y Astropartículas (CNEA, CONICET, UNSAM), Buenos Aires, Argentina
[8] International Center of Advanced Studies and Instituto de Ciencias Físicas, ECyT-UNSAM and CONICET, Campus Miguelete – San Martín, Buenos Aires, Argentina
[9] Laboratorio Atmósfera – Departamento de Investigaciones en Láseres y sus Aplicaciones – UNIDEF (CITEDEF-CONICET), Argentina
[10] Observatorio Pierre Auger, Malargüe, Argentina
[11] Observatorio Pierre Auger and Comisión Nacional de Energía Atómica, Malargüe, Argentina
[12] Universidad Tecnológica Nacional – Facultad Regional Buenos Aires, Buenos Aires, Argentina
[13] University of Adelaide, Adelaide, S.A., Australia
[14] Université Libre de Bruxelles (ULB), Brussels, Belgium
[15] Vrije Universiteit Brussels, Brussels, Belgium
[16] Centro Federal de Educação Tecnológica Celso Suckow da Fonseca, Petropolis, Brazil
[17] Instituto Federal de Educação, Ciência e Tecnologia do Rio de Janeiro (IFRJ), Brazil
[18] Universidade de São Paulo, Escola de Engenharia de Lorena, Lorena, SP, Brazil
[19] Universidade de São Paulo, Instituto de Física de São Carlos, São Carlos, SP, Brazil
[20] Universidade de São Paulo, Instituto de Física, São Paulo, SP, Brazil
[21] Universidade Estadual de Campinas, IFGW, Campinas, SP, Brazil
[22] Universidade Estadual de Feira de Santana, Feira de Santana, Brazil
[23] Universidade Federal de Campina Grande, Centro de Ciencias e Tecnologia, Campina Grande, Brazil
[24] Universidade Federal do ABC, Santo André, SP, Brazil
[25] Universidade Federal do Paraná, Setor Palotina, Palotina, Brazil
[26] Universidade Federal do Rio de Janeiro, Instituto de Física, Rio de Janeiro, RJ, Brazil
[27] Universidade Federal do Rio de Janeiro (UFRJ), Observatório do Valongo, Rio de Janeiro, RJ, Brazil
[28] Universidade Federal Fluminense, EEIMVR, Volta Redonda, RJ, Brazil
[29] Universidad de Medellín, Medellín, Colombia
[30] Universidad Industrial de Santander, Bucaramanga, Colombia

[31] Charles University, Faculty of Mathematics and Physics, Institute of Particle and Nuclear Physics, Prague, Czech Republic
[32] Institute of Physics of the Czech Academy of Sciences, Prague, Czech Republic
[33] Palacky University, Olomouc, Czech Republic
[34] CNRS/IN2P3, IJCLab, Université Paris-Saclay, Orsay, France
[35] Laboratoire de Physique Nucléaire et de Hautes Energies (LPNHE), Sorbonne Université, Université de Paris, CNRS-IN2P3, Paris, France
[36] Univ. Grenoble Alpes, CNRS, Grenoble Institute of Engineering Univ. Grenoble Alpes, LPSC-IN2P3, 38000 Grenoble, France
[37] Université Paris-Saclay, CNRS/IN2P3, IJCLab, Orsay, France
[38] Bergische Universität Wuppertal, Department of Physics, Wuppertal, Germany
[39] Karlsruhe Institute of Technology (KIT), Institute for Experimental Particle Physics, Karlsruhe, Germany
[40] Karlsruhe Institute of Technology (KIT), Institut für Prozessdatenverarbeitung und Elektronik, Karlsruhe, Germany
[41] Karlsruhe Institute of Technology (KIT), Institute for Astroparticle Physics, Karlsruhe, Germany
[42] RWTH Aachen University, III. Physikalisches Institut A, Aachen, Germany
[43] Universität Hamburg, II. Institut für Theoretische Physik, Hamburg, Germany
[44] Universität Siegen, Department Physik – Experimentelle Teilchenphysik, Siegen, Germany
[45] Gran Sasso Science Institute, L'Aquila, Italy
[46] INFN Laboratori Nazionali del Gran Sasso, Assergi (L'Aquila), Italy
[47] INFN, Sezione di Catania, Catania, Italy
[48] INFN, Sezione di Lecce, Lecce, Italy
[49] INFN, Sezione di Milano, Milano, Italy
[50] INFN, Sezione di Napoli, Napoli, Italy
[51] INFN, Sezione di Roma "Tor Vergata", Roma, Italy
[52] INFN, Sezione di Torino, Torino, Italy
[53] Istituto di Astrofisica Spaziale e Fisica Cosmica di Palermo (INAF), Palermo, Italy
[54] Osservatorio Astrofisico di Torino (INAF), Torino, Italy
[55] Politecnico di Milano, Dipartimento di Scienze e Tecnologie Aerospaziali , Milano, Italy
[56] Università del Salento, Dipartimento di Matematica e Fisica "E. De Giorgi", Lecce, Italy
[57] Università dell'Aquila, Dipartimento di Scienze Fisiche e Chimiche, L'Aquila, Italy
[58] Università di Catania, Dipartimento di Fisica e Astronomia "Ettore Majorana", Catania, Italy
[59] Università di Milano, Dipartimento di Fisica, Milano, Italy
[60] Università di Napoli "Federico II", Dipartimento di Fisica "Ettore Pancini", Napoli, Italy
[61] Università di Palermo, Dipartimento di Fisica e Chimica "E. Segrè", Palermo, Italy
[62] Università di Roma "Tor Vergata", Dipartimento di Fisica, Roma, Italy
[63] Università Torino, Dipartimento di Fisica, Torino, Italy
[64] Benemérita Universidad Autónoma de Puebla, Puebla, México
[65] Unidad Profesional Interdisciplinaria en Ingeniería y Tecnologías Avanzadas del Instituto Politécnico Nacional (UPIITA-IPN), México, D.F., México
[66] Universidad Autónoma de Chiapas, Tuxtla Gutiérrez, Chiapas, México
[67] Universidad Michoacana de San Nicolás de Hidalgo, Morelia, Michoacán, México
[68] Universidad Nacional Autónoma de México, México, D.F., México
[69] Universidad Nacional de San Agustin de Arequipa, Facultad de Ciencias Naturales y Formales, Arequipa, Peru
[70] Institute of Nuclear Physics PAN, Krakow, Poland
[71] University of Łódź, Faculty of High-Energy Astrophysics,Łódź, Poland
[72] Laboratório de Instrumentação e Física Experimental de Partículas – LIP and Instituto Superior Técnico – IST, Universidade de Lisboa – UL, Lisboa, Portugal
[73] "Horia Hulubei" National Institute for Physics and Nuclear Engineering, Bucharest-Magurele, Romania
[74] Institute of Space Science, Bucharest-Magurele, Romania
[75] University Politehnica of Bucharest, Bucharest, Romania
[76] Center for Astrophysics and Cosmology (CAC), University of Nova Gorica, Nova Gorica, Slovenia
[77] Experimental Particle Physics Department, J. Stefan Institute, Ljubljana, Slovenia

PoS(ICRC2023)343

[78] Universidad de Granada and C.A.F.P.E., Granada, Spain
[79] Instituto Galego de Física de Altas Enerxías (IGFAE), Universidade de Santiago de Compostela, Santiago de Compostela, Spain
[80] IMAPP, Radboud University Nijmegen, Nijmegen, The Netherlands
[81] Nationaal Instituut voor Kernfysica en Hoge Energie Fysica (NIKHEF), Science Park, Amsterdam, The Netherlands
[82] Stichting Astronomisch Onderzoek in Nederland (ASTRON), Dwingeloo, The Netherlands
[83] Universiteit van Amsterdam, Faculty of Science, Amsterdam, The Netherlands
[84] Case Western Reserve University, Cleveland, OH, USA
[85] Colorado School of Mines, Golden, CO, USA
[86] Department of Physics and Astronomy, Lehman College, City University of New York, Bronx, NY, USA
[87] Michigan Technological University, Houghton, MI, USA
[88] New York University, New York, NY, USA
[89] University of Chicago, Enrico Fermi Institute, Chicago, IL, USA
[90] University of Delaware, Department of Physics and Astronomy, Bartol Research Institute, Newark, DE, USA
[91] University of Wisconsin-Madison, Department of Physics and WIPAC, Madison, WI, USA

—

[a] Louisiana State University, Baton Rouge, LA, USA
[b] also at University of Bucharest, Physics Department, Bucharest, Romania
[c] School of Physics and Astronomy, University of Leeds, Leeds, United Kingdom
[d] now at Agenzia Spaziale Italiana (ASI). Via del Politecnico 00133, Roma, Italy
[e] Fermi National Accelerator Laboratory, Fermilab, Batavia, IL, USA
[f] now at Graduate School of Science, Osaka Metropolitan University, Osaka, Japan
[g] now at ECAP, Erlangen, Germany
[h] Max-Planck-Institut für Radioastronomie, Bonn, Germany
[i] also at Kapteyn Institute, University of Groningen, Groningen, The Netherlands
[j] Colorado State University, Fort Collins, CO, USA
[k] Pennsylvania State University, University Park, PA, USA

Acknowledgments

The successful installation, commissioning, and operation of the Pierre Auger Observatory would not have been possible without the strong commitment and effort from the technical and administrative staff in Malargüe. We are very grateful to the following agencies and organizations for financial support:

Argentina – Comisión Nacional de Energía Atómica; Agencia Nacional de Promoción Científica y Tecnológica (ANPCyT); Consejo Nacional de Investigaciones Científicas y Técnicas (CONICET); Gobierno de la Provincia de Mendoza; Municipalidad de Malargüe; NDM Holdings and Valle Las Leñas; in gratitude for their continuing cooperation over land access; Australia – the Australian Research Council; Belgium – Fonds de la Recherche Scientifique (FNRS); Research Foundation Flanders (FWO); Brazil – Conselho Nacional de Desenvolvimento Científico e Tecnológico (CNPq); Financiadora de Estudos e Projetos (FINEP); Fundação de Amparo à Pesquisa do Estado de Rio de Janeiro (FAPERJ); São Paulo Research Foundation (FAPESP) Grants No. 2019/10151-2, No. 2010/07359-6 and No. 1999/05404-3; Ministério da Ciência, Tecnologia, Inovações e Comunicações (MCTIC); Czech Republic – Grant No. MSMT CR LTT18004, LM2015038, LM2018102, CZ.02.1.01/0.0/0.0/16_013/0001402, CZ.02.1.01/0.0/0.0/18_046/0016010 and CZ.02.1.01/0.0/0.0/17_049/0008422; France – Centre de Calcul IN2P3/CNRS; Centre National de la Recherche Scientifique (CNRS); Conseil Régional Ile-de-France; Département Physique Nucléaire et Corpusculaire (PNC-IN2P3/CNRS); Département Sciences de l'Univers (SDU-INSU/CNRS); Institut Lagrange de Paris (ILP) Grant No. LABEX ANR-10-LABX-63 within the Investissements d'Avenir Programme Grant No. ANR-11-IDEX-0004-02; Germany – Bundesministerium für Bildung und Forschung (BMBF); Deutsche Forschungsgemeinschaft (DFG); Finanzministerium Baden-Württemberg; Helmholtz Alliance for Astroparticle Physics (HAP); Helmholtz-Gemeinschaft Deutscher Forschungszentren (HGF); Ministerium für Kultur und Wissenschaft des Landes Nordrhein-Westfalen; Ministerium für Wissenschaft, Forschung und Kunst des Landes Baden-Württemberg; Italy – Istituto Nazionale di Fisica Nucleare (INFN); Istituto Nazionale di Astrofisica (INAF); Ministero dell'Universitá e della Ricerca (MUR); CETEMPS Center of Excellence; Ministero degli Affari Esteri (MAE), ICSC Centro Nazionale di Ricerca in High Performance Computing, Big Data

and Quantum Computing, funded by European Union NextGenerationEU, reference code CN_00000013; México – Consejo Nacional de Ciencia y Tecnología (CONACYT) No. 167733; Universidad Nacional Autónoma de México (UNAM); PAPIIT DGAPA-UNAM; The Netherlands – Ministry of Education, Culture and Science; Netherlands Organisation for Scientific Research (NWO); Dutch national e-infrastructure with the support of SURF Cooperative; Poland – Ministry of Education and Science, grants No. DIR/WK/2018/11 and 2022/WK/12; National Science Centre, grants No. 2016/22/M/ST9/00198, 2016/23/B/ST9/01635, 2020/39/B/ST9/01398, and 2022/45/B/ST9/02163; Portugal – Portuguese national funds and FEDER funds within Programa Operacional Factores de Competitividade through Fundação para a Ciência e a Tecnologia (COMPETE); Romania – Ministry of Research, Innovation and Digitization, CNCS-UEFISCDI, contract no. 30N/2023 under Romanian National Core Program LAPLAS VII, grant no. PN 23 21 01 02 and project number PN-III-P1-1.1-TE-2021-0924/TE57/2022, within PNCDI III; Slovenia – Slovenian Research Agency, grants P1-0031, P1-0385, I0-0033, N1-0111; Spain – Ministerio de Economía, Industria y Competitividad (FPA2017-85114-P and PID2019-104676GB-C32), Xunta de Galicia (ED431C 2017/07), Junta de Andalucía (SOMM17/6104/UGR, P18-FR-4314) Feder Funds, RENATA Red Nacional Temática de Astropartículas (FPA2015-68783-REDT) and María de Maeztu Unit of Excellence (MDM-2016-0692); USA – Department of Energy, Contracts No. DE-AC02-07CH11359, No. DE-FR02-04ER41300, No. DE-FG02-99ER41107 and No. DE-SC0011689; National Science Foundation, Grant No. 0450696; The Grainger Foundation; Marie Curie-IRSES/EPLANET; European Particle Physics Latin American Network; and UNESCO.